J MATER SCI 41 (2006) 2885–2893

# Fracture surface topography and fracture mechanism in austenitic SUS316 steel plates fatigued by repeated bending

M. TANAKA*
*Professor, Research Institute of Materials and Resources, Department of Mechanical Engineering, Faculty of Engineering and Resource Science, Akita University, 1-1 Tegatagakuen-cho, Akita 010-8502, Japan*
*E-mail: tanaka@mech.akita-u.ac.jp*

Y. KIMURA
*Nippon Software Company Ltd., 31-11 Sakuragaoka-cho, Shibuya-ku, Tokyo 150-8577, Japan*

J. TAGUCHI
*Student of Graduate School, Department of Mechanical Engineering, Akita University, Japan*

R. KATO
*Technical Assistant, Department of Mechanical Engineering, Akita University, 1-1 Tegatagakuen-cho, Akita 010-8502, Japan*

**Published online:** 20 March 2006

Fatigue experiments were carried out using the austenitic SUS316 steel plates (the average grain diameter is about $1.3 \times 10^{-5}$ m) by repeated bending. The three-dimensional fatigue fracture surfaces were then reconstructed using stereo pairs of scanning electron micrographs by the stereo matching method. Striations were observed on the stage II fatigue fracture surface, while fine slip steps were found on the stage I fatigue fracture surface. The averaged value of the fractal dimension of stage I fracture surface was about 2.2 and was almost the same as that of stage II fracture surface when the fractal dimension was measured in the length scale range smaller than about one grain-boundary length (about $8 \times 10^{-6}$ m). This may be attributed to the fact that both fracture surfaces were formed by the same mechanism, namely, slipping-off. According to the two-dimensional fractal analysis, both stage I and stage II fatigue fracture surfaces did not exhibit anisotropy in the length scale range of the fractal analysis smaller than about one grain-boundary length in the SUS316 steel. The fractal dimension of the fatigue fracture surface increased with decreasing the magnification of images when the maximum length scale of the fractal analysis was extended to the size of analyzed area. Magnification dependence of the fractal dimension was associated with large steps and ledges, which were not "typical" fractals. 

## 1. Introduction

Fractal geometry created by Mandelbrot has been applied to the interpretation of physical phenomena including fracture of materials [1–3]. Geometrical features of fracture surfaces in materials can be quantitatively described by the fractal dimension [2–4]. However, the fractal dimension depends not only on the fracture mechanism and the microstructures [3, 4] but also on the size of analyzed area on a fracture surface [5]. Yamagiwa et al. [6] examined the relationship between the magnification of observation and the fractal dimension of the fracture surface in a TiAl. They reported that the fractal dimension of the fracture surface decreased below a certain scale of observation, which was characteristic to fracture, although the values of the fractal dimension seem to be considerably high (from about 2.5 to about

*Author to whom all correspondence should be addressed.
0022-2461 
DOI: 10.1007/s10853-005-5160-0

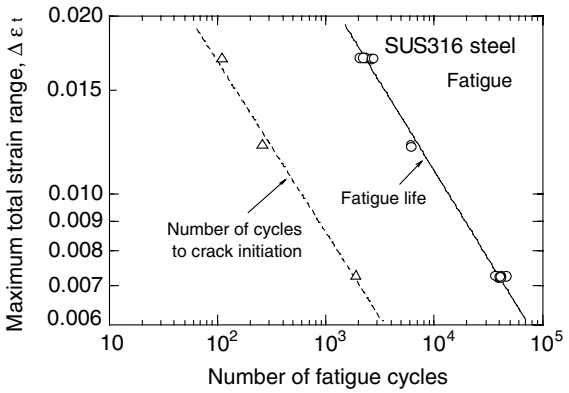


*Figure 1* Fatigue life and number of cycles to crack initiation in the SUS316 steel plates fatigued by repeated bending.

2.9). Their result implies that the fractal dimension of the fracture surface decreases with increasing magnification of images. It is known that fracture surfaces show a multi-fractal behavior depending on the scale length range of the fractal analysis, which is associated with characteristic microstructures on the fracture surface of materials [4, 7, 8]. Further, it is not uncommon that a given fracture surface has a self-similarity in a certain length scale range, while the fracture surface does not show a scaling of the topographical features in other length scale ranges [9]. Therefore, the fractal dimension estimated in a given length scale range may represent a certain microstructure with a similar size range on a given fracture surface [4].

In this study, three-dimensional fracture surfaces were reconstructed by the stereo matching method on the fatigued specimens of the austenitic SUS316 steel [10, 11]. The fractal dimension of the three-dimensional fatigue fracture surface was estimated by the box-counting method [12]. The dependence of the fractal dimension on the magnification of images was then examined in relation to the characteristic microstructures and the length scale range of the fractal analysis. Two-dimensional fractal analysis of the fatigue fracture surface profiles was also carried out to examine whether the fatigue fracture surfaces have anisotropy or not. The result of the two-dimensional fractal analysis was compared with that of the three-dimensional fractal analysis. Correlations between the fracture mechanisms and the fracture patterns were discussed on the basis of the experimental results.

## 2. Experimental procedure and analytical method

Fatigue experiments were carried out using the austenitic SUS316 steel plates (Fe–0.06 wt%C–16.80 wt%Cr–10.20 wt%Ni–2.11 wt%Mo) (the average grain diameter is about $1.3 \times 10^{-5}$ m and the one grain-boundary length is about $8 \times 10^{-6}$ m) by repeated bending at the maximum total strain range ($\Delta\varepsilon_t$) from 0.00723 to 0.0169 on the specimen surface [13, 14]. The frequency of the fatigue cycling was 0.7 Hz. Fracture surfaces of the fatigued specimens were observed by a scanning electron microscope (SEM), while crack initiation on the specimen surface was confirmed by optical microscope. Stereo pairs of scanning electron micrographs were taken on the same spot in a specimen at various magnifications in the range from about 74 to about 8100 times in SEM, and were taken into a personal computer as bitmap files of 256 grey scale levels. More than 520 grains were involved in the images taken at the lowest magnification. Three-dimensional fatigue fracture surfaces were then reconstructed using the stereo pairs of SEM images by the stereo matching method [10, 11]. The stereo matching method used in this study gives a favorable result of the three-dimensional image reconstruction with a reasonable accuracy in a relatively short time. The details of the stereo matching method are shown in the references [10, 11]. The fractal dimension of the three-dimensional fatigue fracture surface in the SUS316 steel was estimated by the box-counting method using the height data generated from three-dimensional image reconstruction at different magnifications [12]. The fractal dimension (D) can be calculated from the relationship between the number of

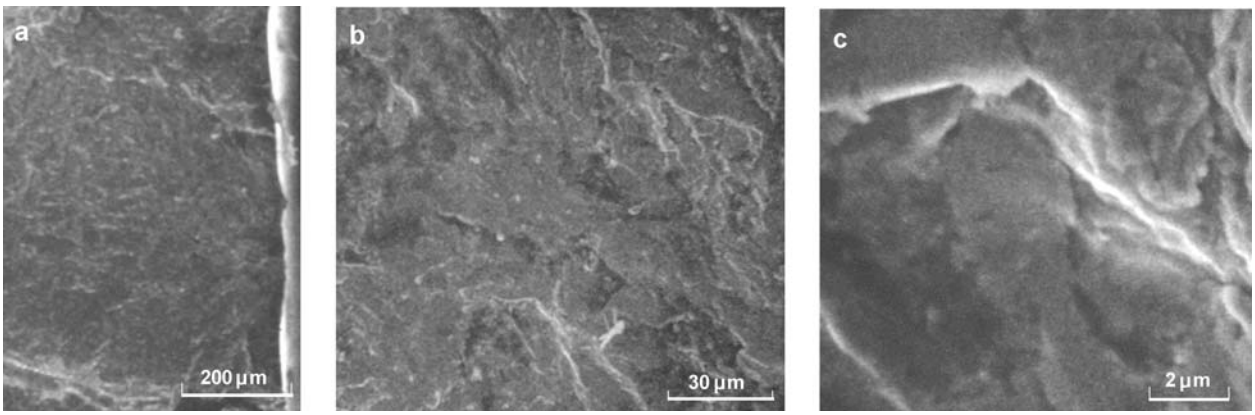


*Figure 2* Stage I fatigue fracture surfaces in the SUS316 steel ($\Delta\varepsilon_t = 0.0169$). a. $M = 81$ times, b. $M = 810$ times, c. $M = 8100$ times (M: magnification of images).

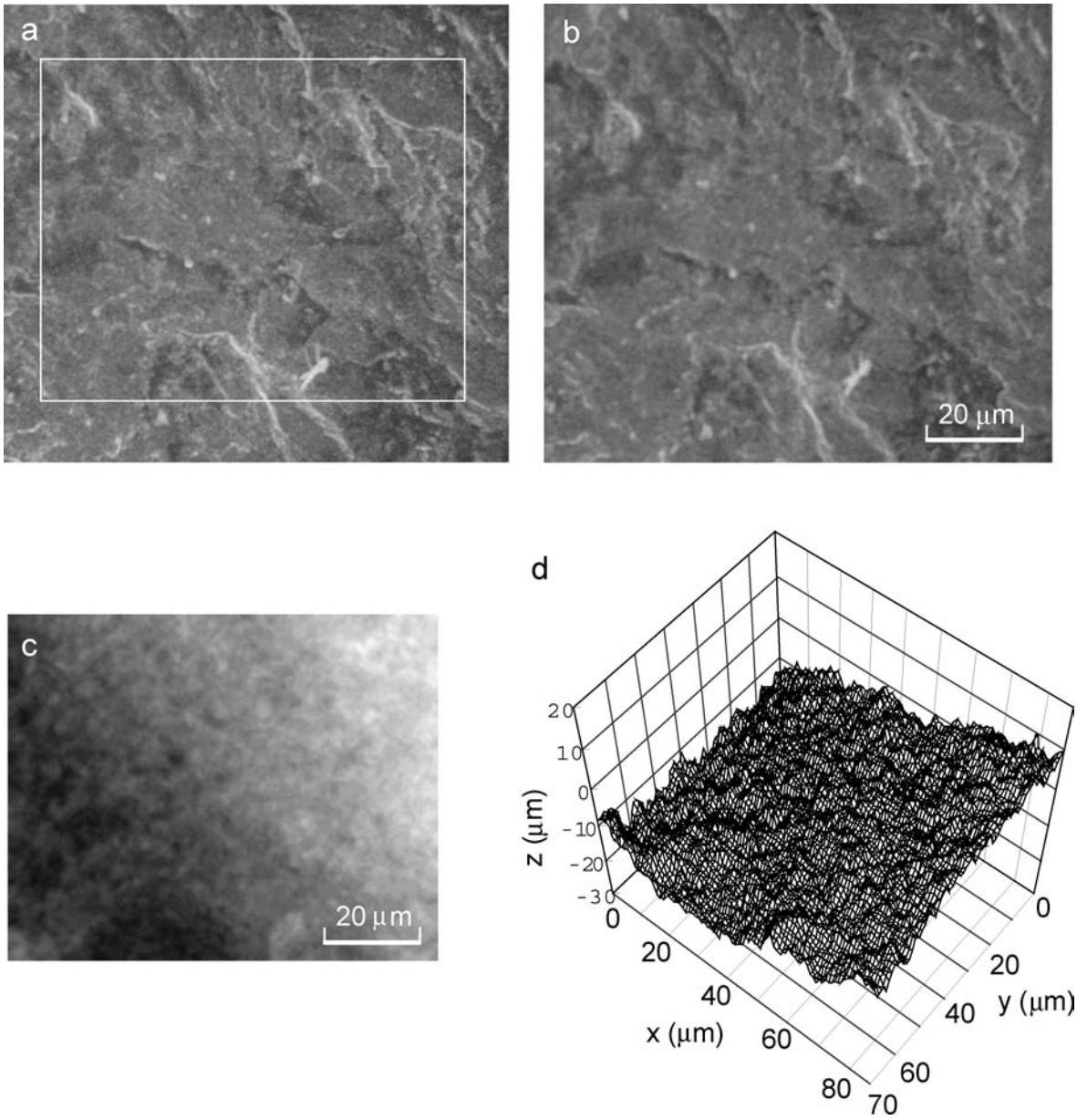


*Figure 3* An example of the three-dimensional image reconstruction in the SUS316 steel (stage I fatigue fracture surface, $\Delta\varepsilon_t = 0.0169$). a. basic image, b. tilted image (tilted by 10 deg.), c. height image d. bird's-eye view.

boxes (N) covering the fracture surface and the box size ($r$) ($N \propto r^{-D}$). Two-dimensional fractal analysis was also carried out on the fracture surface profiles of the fatigued specimens in both planes in parallel with and transverse to the crack growth direction. The fractal dimension of the fatigue fracture surface profile was estimated on the preprocessed images of the fracture surface profiles by using the computer program of the box-counting method that was used in the previous study [13]. The fractal dimension ($D'$) can be obtained from the relationship between the length of the fracture surface profile (L) and the length scale of the fractal analysis ($r'$) ($L \propto r'^{1-D'}$). The fractal dimension of the fatigue fracture surface profile was the averaged value over about 6 to 12 fracture surface profiles (each fracture surface profile involves about 13 grains).

## 3. Results and discussion

### 3.1. Microstructural features on fatigue fracture surfaces

#### *3.1.1. Stage I fatigue fracture surface*

Fig. 1 shows the fatigue life and the number of cycles to crack initiation in the SUS316 steel plates fatigued by repeated bending. Fatigue crack initiation occurred within the grains in the early stage of fatigue. As shown in the figure, the number of cycles to crack initiation is below about 5% of the fatigue life. Therefore, most of the fatigue life is occupied by the growth and linkage of fatigue cracks, namely, by the formation of fatigue fracture surface in this steel.

Fig. 2 shows the stage I fatigue fracture surfaces in the SUS316 steel ($\Delta\varepsilon_t = 0.0169$). These scanning electron micrographs are the basic images for the stereo matching

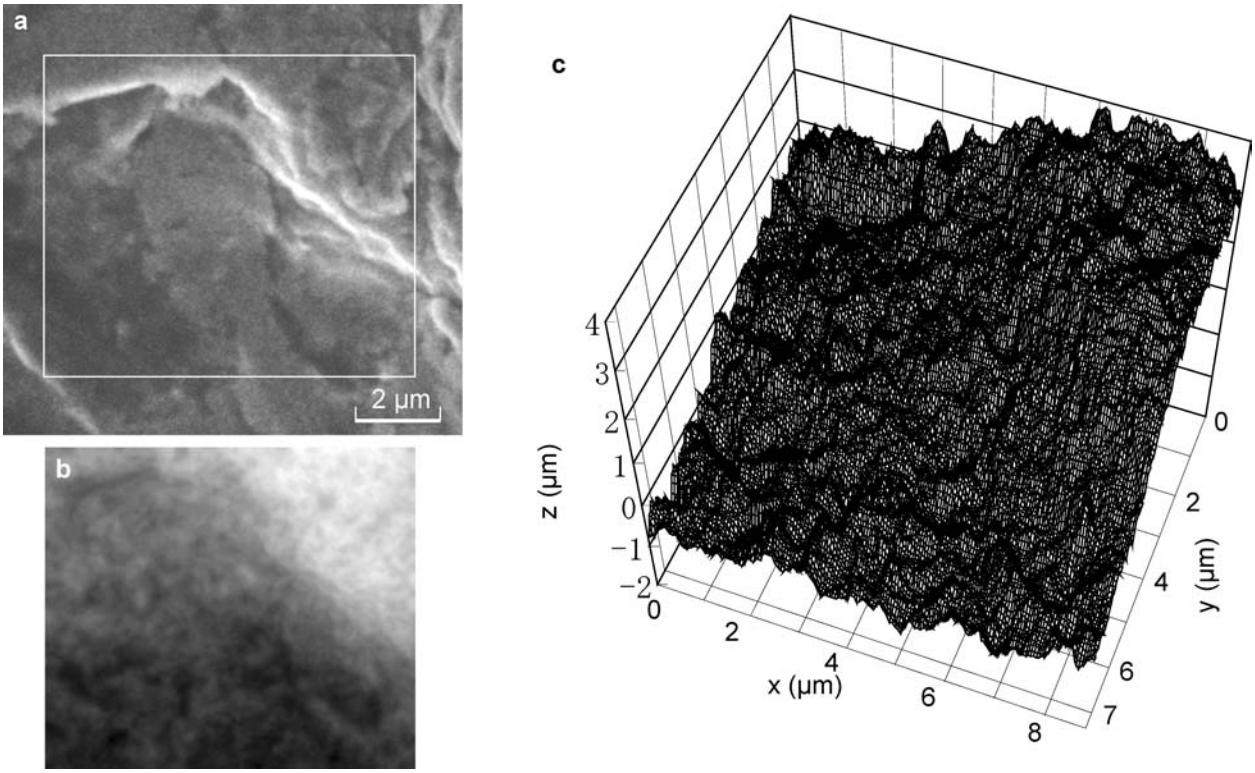


*Figure 4* High magnification image of stage I fatigue fracture surface in the SUS316 steel ($\Delta\varepsilon_t = 0.0169$). a. computed area (765 × 615 in pixel), b. height image, c. bird's-eye view of a.

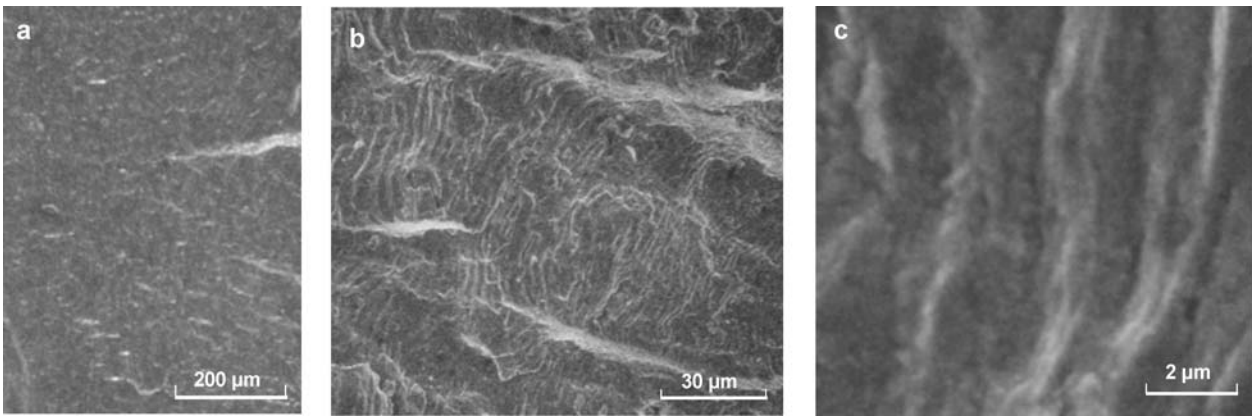


*Figure 5* Stage II fatigue fracture surfaces in the SUS316 steel ($\Delta\varepsilon_t = 0.0169$). a. $M = 81$ times, b. $M = 810$ times, c. $M = 8100$ times (M: magnification of images).

method and the crack growth direction is approximately from right to left in these photographs. The stage I fatigue fracture surface is relatively flat and featureless at the lowest magnification except large steps and ledges which are equal to or larger than one grain-boundary length (about $8 \times 10^{-6}$ m) (Fig. 2a) [13, 14]. However, fine slip steps of the sizes smaller than one grain-boundary length are visible in addition to large steps and ledges at the intermediate magnification (Figs. 2b). These patterns were commonly observed on the stage I fatigue fracture surface of the specimens fatigued under different conditions ($\Delta\varepsilon_t$). A large step can be seen at the upper part of the micrograph taken at the highest magnification (Fig. 2c).

Fig. 3 shows an example of the three-dimensional image reconstruction in the SUS316 steel (stage I fatigue fracture surface, $\Delta\varepsilon_t = 0.0169$). The height data of the fracture surface are obtained by the stereo matching method using the basic image (Fig. 3a, the same as Fig. 2b) and the tilted image (tilted the specimen by 10 deg., Fig. 3b). The computed area by the stereo matching method is shown in Fig. 3a. The height data are displayed as the height image of 256 grey scale levels in Fig. 3c. The higher part of the fracture surface is shown by the brighter region in the height image. The height data can also be displayed as the bird's-eye view (three-dimensional image) in Fig. 3d. Large steps and ledges as well as fine steps

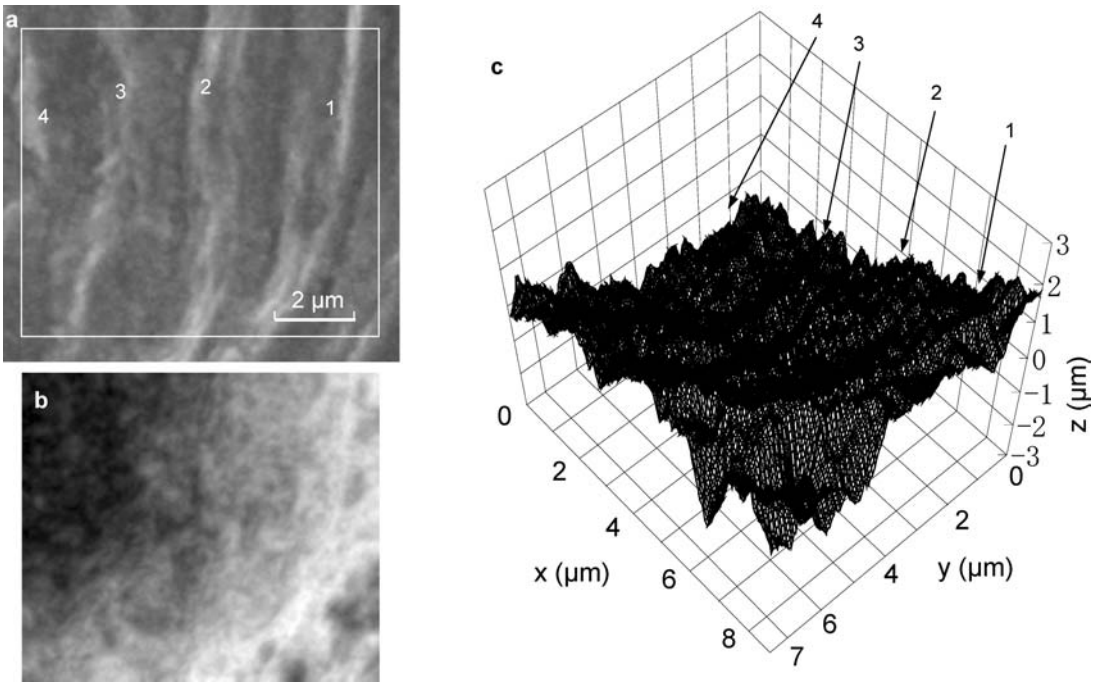


*Figure 6* High magnification image of stage II fatigue fracture surface in the SUS316 steel ($\Delta\varepsilon_t = 0.0169$). a. computed area (769 × 663 in pixel) (the number shows the peak of the striation pattern), b. height image, c. bird's-eye view of a.

are visible in the bird's-eye view. Fig. 4 shows the high magnification image of stage I fatigue fracture surface in the SUS316 steel ($\Delta\varepsilon_t = 0.0169$). The computed area is shown by a square of 765 × 615 in pixel in Fig. 4a. The upper right part is the higher region of the fracture surface and exhibits the brighter contrast in the height image (Fig. 4b). As known from the bird's-eye view (Fig. 4c), many fine steps are imposed with a large step on the fracture surface. The height of the large step is about 5 micron meter. The fine steps may be slip steps formed by dislocation slip in the grains during stage I fatigue.

### 3.1.2. Stage II fatigue fracture surface

Fig. 5 shows the stage II fatigue fracture surfaces in the SUS316 steel ($\Delta\varepsilon_t = 0.0169$). These scanning micrographs are also used as the basic images for the stereo matching method in this study. The crack growth direction is approximately from right to left in these micrographs. Only large steps and ledges, which are equal to or larger than one grain-boundary length in size, are visible at the lowest magnification (Fig. 5a), while striations as well as large steps and ledges can be seen at the intermediate magnification (Fig. 5b) [13, 14]. Fig. 5c is an enlarged photograph of striations observed in the upper right part of Fig. 5d. Large steps or ledges are not observed in this figure. Similar patterns were observed on the fracture surface of the specimen fatigued at $\Delta\varepsilon_t = 0.00723$. Fig. 6 shows the high magnification image of stage II fatigue fracture surface in the SUS316 steel ($\Delta\varepsilon_t = 0.0169$). The computed area and the peak number of the striations are shown in Fig. 6a. Peaks and valleys of these striations can also be recognized in the height image (Fig. 6b). As shown in Fig. 6c, the striations are well reproduced by the stereo matching method in this study. The striation spacing is a few micron meters and is similar in size to the height difference between peaks and valleys, although striations exhibit complicated patterns like groups of mountains.

Table I lists the spacing ranges of striations, slip steps and large steps and ledges observed on the fatigue fracture surfaces of the SUS316 steel. Microstructural features in the size ranges smaller than one grain-boundary length (about $8 \times 10^{-6}$ m) are fine slip steps in the stage I fatigue fracture surface and striations in the stage II fatigue fracture surface. Large steps and ledges which are equal to or larger than one grain-boundary length, are visible in both stage I and stage II fatigue fracture urfaces. Thus, detectable microstructures depend on the scale of measurements or the magnification of images on these fracture surfaces.

TABLE I Spacing ranges of striations, slip steps, and large steps and ledges observed on the fracture surfaces in the fatigued specimens of the SUS316 steel

| | Stage I | | Stage II | |
|---|---|---|---|---|
| $\Delta\varepsilon_t$ | Slip steps ($10^{-6}$ m) | Large steps and ledges ($10^{-6}$ m) | Striations ($10^{-6}$ m) | Large steps and ledges ($10^{-6}$ m) |
| 0.00723 | 0.6 to 6 | 9 to 56 | 0.4 to 5 | 8 to 60 |
| 0.0169 | 0.5 to 5 | 8 to 56 | 0.5 to 6 | 8 to 66 |

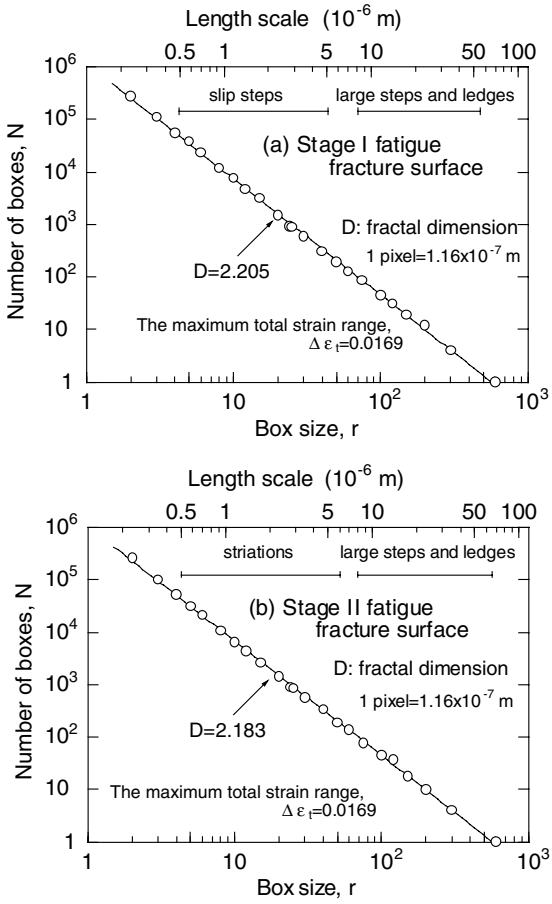


*Figure 7* Results of the three-dimensional fractal analysis on the stage I and stage II fatigue fracture surfaces in the SUS316 alloy ($\Delta\varepsilon_t = 0.0169$).

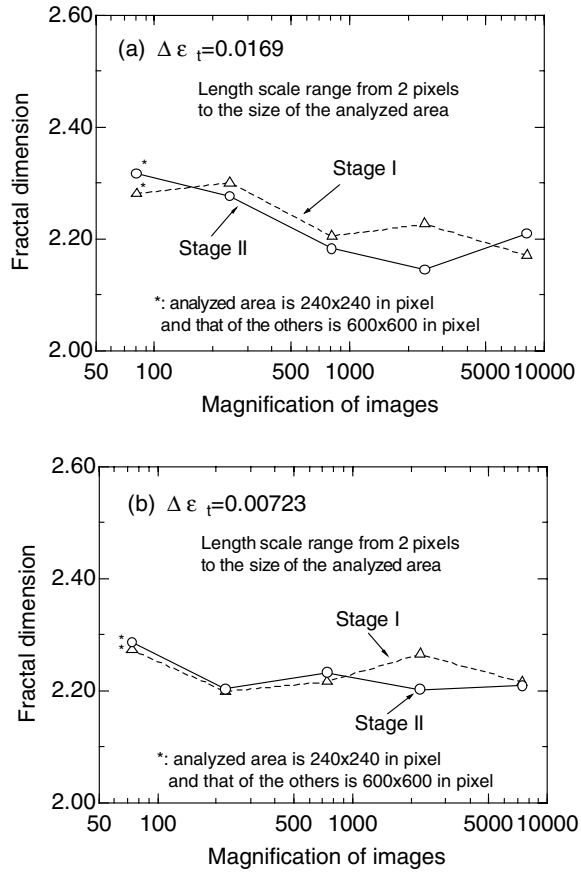


*Figure 8* The relationship between the fractal dimension of the fatigue fracture surface and the magnification of the analyzed images in the SUS316 steel.

## 3.2. Three-dimensional fractal analysis

### *3.2.1. Relationship between the fractal dimension and the magnification of images*

Fig. 7 shows the results of the three-dimensional fractal analysis on the stage I and stage II fatigue fracture surfaces in the SUS316 steel ($\Delta\varepsilon_t = 0.0169$). The fractal dimension of the three-dimensional fatigue fracture surface was estimated in the length scale range from two pixels to the size of the analyzed area (600 pixels). The size ranges of characteristic microstructures are also shown in the figure. The fractal dimension of the stage I fatigue fracture surface may represent slip steps, and large steps and ledges on the fracture surface, because the fractal dimension was estimated in the length scale range including the size ranges of both microstructures (Figs. 7a). The fractal dimension of the stage II fatigue fracture surface can be correlated to striations, and large steps and ledges (Figs. 7b).

Fig. 8 shows the relationship between the fractal dimension of the fatigue fracture surface and the magnification of the analyzed images in the SUS316 steel. The analyzed area is 240 × 240 in pixel for the image of the lowest magnification and 600 × 600 in pixel for the other images. The length scale range of the fractal analysis is from two pixels to the size of the analyzed area (240 or 600 pixels). Both fractal dimensions of the stage I and stage II fatigue fracture surfaces tend to decrease with increasing the magnification of images in the specimen fatigued at $\Delta\varepsilon_t = 0.0169$ (Fig. 8a). The fractal dimension in the stage I and stage II fatigue fracture surfaces is largest on the image of the lowest magnification in the specimens fatigued at $\Delta\varepsilon_t = 0.00723$, although magnification dependence of the fractal dimension is not remarkable in this case (Figs. 8b). As known from Fig. 7, the magnification dependence of the fractal dimension is related to microstructures involved in the analyzed images. Therefore, it is important to estimate the fractal dimension in the length scale range that is associated with the size range of a microstructure [4, 7, 8].

### *3.2.2. Relationship between fractal dimension and microstructures*

Fig. 9 shows the fractal dimension of the fatigue fracture surfaces estimated in the length scale range smaller than about one grain-boundary length in the SUS316 steel. The fractal dimension of the stage I fatigue fracture surface represents fine slip steps on the fracture surface, while the fractal dimension of the stage II fatigue fracture surface

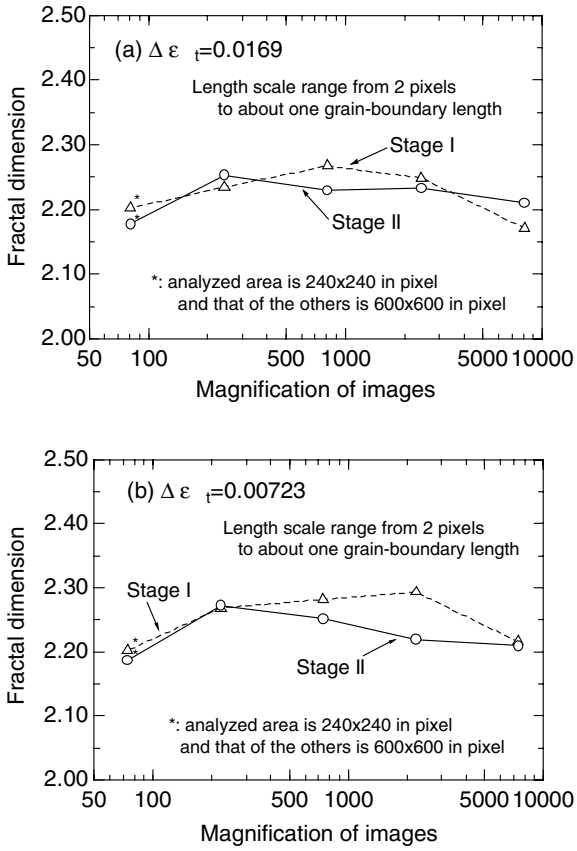


*Figure 9* The fractal dimension of the fatigue fracture surfaces estimated in the length scale range smaller than about one grain-boundary length in the SUS316 steel.

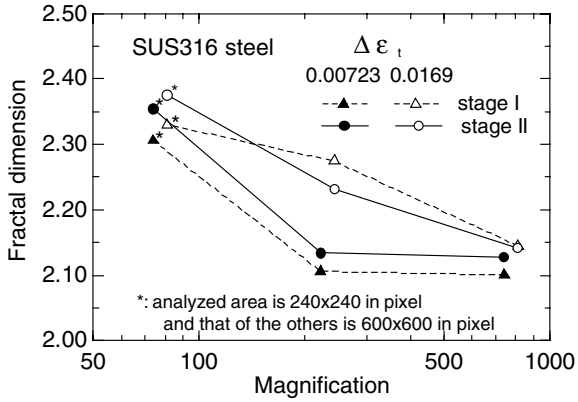


*Figure 10* The "tentative" fractal dimension of the fatigue fracture surface estimated in the length scale larger than about one grain-boundary length in the SUS316 steel.

can be correlated with striations [13]. The fractal dimension essentially does not depend on the magnification of images in all cases. The averaged value of the fractal dimension is about 2.22 for both stage I and stage II fatigue fracture surfaces in the specimen fatigued at $\Delta\varepsilon_t = 0.0169$ (Fig. 9a), and is about 2.25 for stage I fatigue fracture surface and about 2.23 for stage II fatigue fracture surface in the specimen fatigued at $\Delta\varepsilon_t = 0.00723$ (Fig. 9b). It is interesting to note that both stage I and stage II fatigue fracture surfaces have almost the same fractal dimension, in spite of the difference in the characteristic fracture patterns. This may indicate that both stage I and stage II fatigue fracture surfaces are formed by the common fracture mechanism, namely, slipping-off. The value of the fractal dimension was much the same for the specimens fatigued under different maximum total strain ranges ($\Delta\varepsilon_t$).

On the contrary, the fractal dimension has a magnification dependence of images in the length scale larger than about one grain-boundary length. Fig. 10 shows the "tentative" fractal dimension of the fatigue fracture surface estimated in the length scale range larger than about one grain-boundary length in the SUS316 steel. The length scale range, in which the fractal dimension is estimated, is associated with the sizes of large steps and ledges on the fatigue fracture surface. The fractal dimensions of both stage I and stage II fatigue fracture surfaces tend to decrease with increasing magnification of images. This means that both fatigue fracture surfaces do not have a unique fractal dimension in the length scale larger than about one grain-boundary length. This may indicate that large steps and ledges observed on the fatigue fracture surface are not "typical" fractals like fine slip steps or striations, which have a unique fractal dimension of about 2.2. These large steps and ledges may have a self-affine nature [15], although further study is required. Thus, the involvement of such microstructures may lead to the magnification dependence of the fractal dimension on the fatigue fracture surfaces of the SUS316 steel.

### 3.3. Two-dimensional fractal analysis

Fig. 11 shows the stage II fatigue fracture surface profiles in the SUS316 steel ($\Delta\varepsilon_t = 0.0169$). Many small steps are visible in addition to much larger steps in both fracture surface profiles in the plane in parallel to the crack growth direction (Fig. 11a) and in the plane transverse to the crack growth direction (Fig. 11b). As described above, the length scale range smaller than about one grain-boundary length, in which the fractal dimension of the fatigue fracture surface is measured, corresponds to the size range of striations or fine slip steps, which characterizes the fatigue fracture surfaces. Therefore, two-dimensional fractal analysis was made in this smaller length scale range [13]. Fig. 12 shows the fractal dimensions of the fracture surface profiles corresponding to Figs 11a and b in the stage II fatigue ($\Delta\varepsilon_t = 0.0169$). The fatigue fracture surface profiles show similar values of the fractal dimension in both planes in parallel with and transverse to the crack growth direction. Table II lists the fractal dimension of the fatigue fracture surface profile, D′, in the SUS316 steel. There is essentially no significant difference in the fractal dimension of the fatigue fracture surface profile between both planes in the stage I and stage II fatigue fracture surfaces of the specimens fatigued under the same condition, if the standard deviation ($\sigma$) of the fractal dimension is taken into account. It is interesting to note that there is

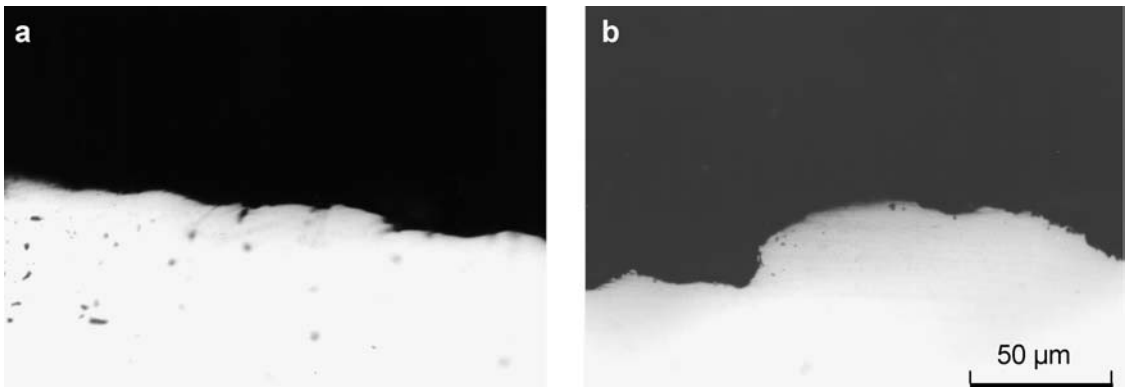


*Figure 11* Stage II fatigue fracture surface profiles in the SUS316 steel ($\Delta\varepsilon_t = 0.0169$). a. in the plane in parallel with the crack growth direction, b. in the plane transverse to the crack growth direction.

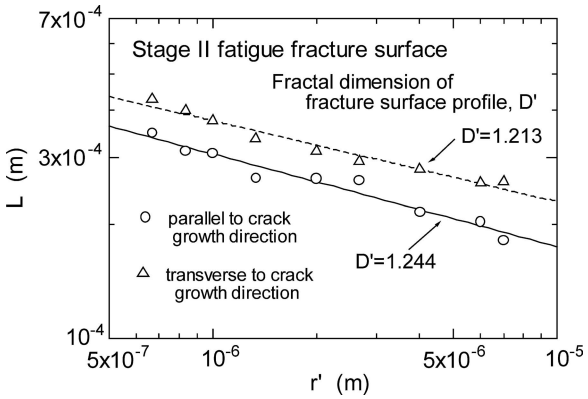


*Figure 12* The fractal dimensions of the fracture surface profiles corresponding to Figs 11a and b in the stage II fatigue of the specimen at $\Delta\varepsilon_t = 0.0169$ (L: the length of the fracture surface profile; r': the length scale of the fractal analysis).

TABLE II The fractal dimension of the fatigue fracture surface profile, D′, in the SUS316 steel

| $\Delta\varepsilon_t$ | Stage I | | Stage II | |
|---|---|---|---|---|
| 0.0169 | P | 1.214 ($\sigma = 0.0567$) | P | 1.221 ($\sigma = 0.0606$) |
| | T | 1.246 ($\sigma = 0.0430$) | T | 1.259 ($\sigma = 0.0446$) |
| 0.00723 | P | 1.227 ($\sigma = 0.0426$) | P | 1.231 ($\sigma = 0.0470$) |
| | T | 1.243 ($\sigma = 0.0445$) | T | 1.262 ($\sigma = 0.0253$) |

P: the fractal dimension in the plane in parallel with the crack growth direction; T: the fractal dimension in the plane transverse to the crack growth direction; $\sigma$: the standard deviation of the fractal dimension.

almost no difference in the fractal dimension between both planes in parallel with and transverse to the crack growth direction even in the stage II fatigue fracture surface with striations. Both fractal dimensions of the stage I and stage II fatigue fracture surface profiles give almost the same value under two different fatigue conditions. Thus, the fatigue fracture surfaces did not exhibit anisotropy in the length scale range of the fractal analysis smaller than about one grain-boundary length in the SUS316 steel.

## 4. Conclusions

The fractal dimension of the fracture surface was estimated by the box-counting method using the height image that was generated by the three-dimensional image reconstruction on the fatigue fracture surface of the austenitic SUS316 steel formed by repeated bending. Striations were characteristic patterns of the stage II fatigue fracture surface, while fine slip steps were observed on the stage I fatigue fracture surface. However, both fractal dimensions of the stage I and stage II fatigue fracture surfaces exhibit almost the same value, about 2.2 on the average, under two different fatigue conditions when the fractal dimension of the three-dimensional fatigue fracture surface was estimated in the length scale range smaller than about one grain-boundary length (about $8 \times 10^{-6}$ m). The results showed that both stage I and stage II fatigue fracture surfaces were formed by the same fracture mechanism, namely, slipping-off. In the two-dimensional fractal analysis, there was essentially no significant difference in the fractal dimension of the fatigue fracture surface profile between both planes in parallel with and transverse to the crack growth direction in both stage I and stage II fatigue fracture surfaces. Thus, the fatigue fracture surfaces did not exhibit anisotropy in the length scale range of the fractal analysis smaller than about one grain-boundary length in the SUS316 steel. The fractal dimension tended to decrease with increasing magnification of images when the fractal dimension was estimated in the length scale range extended to the size of analyzed area. Magnification dependence of the fractal dimension was associated with large steps and ledges, which were not "typical" fractals like fine slip steps or striations and did not have a unique fractal dimension.

## Acknowledgments

The authors thank The Iron and Steel Institute of Japan (Tekkou-Kenkyu-Shinnkou-Josei) for financial support.

## References

1. B. B. MANDELBROT, "The Fractal Geometry of Nature", translated by H. Hironaka (Nikkei Science, Tokyo, 1985) p. 6.

2. B. B. MANDELBROT, D. E. PASSOJA and A. J. PAULLAY, *Nature* **308** (1984) 721.
3. V. Y. MILMAN, N. A. STELMASHENKO and R. BLUMENFELD, *Progress in Mater. Sci.* **38** (1994) 425.
4. R. H. DAUSKARDT, F. HAUBENSAK and R. O. RITCHIE, *Acta. Metall.* **38** (1990) 142.
5. N. ALMQVIST, *Surface Science* **355** (1996) 221.
6. K. YAMAGIWA, S. SAKAI and T. YOKOBORI, *J. Japan Soc. Strength Frac. Mater.* **35** (2001) 53.
7. M. TANAKA and Z. METALLKD **84** (1993) 697.
8. M. TANAKA, *J. Mater. Sci.* **28** (1993) 5753.
9. D. HULL, "Fractography" (Cambridge University Press, Cambridge, 1999), 12.
10. M. TANAKA, Y. KIMURA, L. CHOUANINE, J. TAGUCHI and R. KATO, *ISIJ International.* **43** (2003) 1453.
11. Y. KIMURA, M. TANAKA and R. KATO, *ibid.* **44** (2004) 1276.
12. M. TANAKA, Y. KIMURA, L. CHOUANINE, R. KATO and J. TAGUCHI, *J. Mater. Sci. Lett.* **22** (2003) 1279.
13. M. TANAKA, A. KAYAMA and R. KATO, *ibid.* **18** (1999) 107.
14. M. TANAKA, R. KATO and A. KAYAMA, *J. Mater. Sci.* **37** (2002) 3945.
15. B. B. MANDELBROT, "Dynamics of Fractal Surfaces, Chapter 2. Self-Affine Geometry," edited by F. Family and T. Vicsek (World Scientific, Singapore, 1991) p. 5.

*Received 28 June 2004*
*and accepted 22 June 2005*